

## ***H*-Field Contribution to the Electromagnetic Energy Deposition in Tissues Similar to the Brain But Containing Ferrimagnetic Particles, during Use of Face-Held Radio Transceivers**

Simona Miclaus<sup>1, \*</sup>, Mihaela Racuciu<sup>2</sup>, and Paul Bechet<sup>1</sup>

**Abstract**—A portable radio transceiver with rubber ducky antenna emitting at 446 MHz with an output power of 5 W was considered as near-field source of electric ( $E$ ) and magnetic ( $H$ ) field components when being used in the proximity of the user’s face. By taking into account the significant content of ferrimagnetic nanoparticles recently identified to reside in the human brain, we assessed the specific absorption rate (SAR) of energy deposition due to  $H$ -component penetrating a presumptive forebrain.  $H$ -component SAR contribution to the total SAR is for the first time estimated in such a case, based on an original idea inspired from knowledge on magnetic fluids hyperthermia.

### **1. MAGNETIC PROPERTIES OF BRAIN TISSUE AND THE APPROACH OF ELECTROMAGNETIC DOSIMETRY**

In 1992 Kirschvink and colleagues reported, for the first time, the presence of magnetic material in the human brain in the form of tiny crystals of magnetite, which were hypothesized to have biogenic origin [1]. Some other human organs were later proved to contain biogenic ferrimagnetic materials: liver, spleen, pancreas, heart and lungs. Recently, all these tissues were carefully investigated by Sant’Ovaia et al. [2] who reported presence of magnetic biominerals in various proportions and locations in human body tissues and classified them taking into account their mean magnetic susceptibility and their saturation isothermal remanent magnetization.

In the present, scientific evidence indicates the presence of six iron oxides in human brain tissue [3], and oxides are well characterized. However, the exact role of magnetic minerals in tissues remains unclear after decades of study. In the case of the brain, a few hypotheses exist — it seems that magnetite crystals are located in neurons, and they might be involved in the storage of memory. A very recent hypothesis [4] sustains that magnetite deposited in the outer membranes of the brain could even act as a shield against external electromagnetic radiation.

Up to the end of 2014, the knowledge about magnetite distribution in the brain indicated that pia- and dura-mater outer layers of human brain contain  $10^8$  magnetite nanocrystals per gram, organized in clusters, while other brain tissues contain about  $5 \times 10^6$  nanocrystals per gram [4]. Dimensions of biogenic magnetite crystals are in the range of 30–70 nm, and their shapes are angular, cubo-octahedral or prismatic.

In September 2016, a surprising discovery was reported by Maher and coworkers [5]. They identified a very high quantity of magnetic crystals in human brain tissues — which had an external, environmental origin. It seems that anthropogenic magnetic particles, which can be generated by some professional activities, are able to penetrate in the head by respiratory tract and to store in the brain, adding to the

---

*Received 1 January 2017, Accepted 12 February 2017, Scheduled 1 March 2017*

\* Corresponding author: Simona Miclaus (simo.miclaus@gmail.com).

<sup>1</sup> Department of Technical Sciences, “Nicolae Balcescu” Land Forces Academy, Sibiu, Romania. <sup>2</sup> Department of Environmental Sciences and Physics, Faculty of Sciences, “Lucian Blaga” University of Sibiu, Romania.

afore-discovered biogenic magnetite. The shape of exogenous magnetite particles discovered in human brains is different — being rounded, and the “nanospheres” may present fused surface textures. The concentrations are in the range 0.2–12  $\mu\text{g}$  of magnetic material per gram of dry tissue, and the diameters are spread between 10–150 nm. Moreover, in December 2016, the authors of [6] have shown that a combination of two specific methods offers a unique possibility to study and properly characterize the iron accumulation in the human brain. They also formulated the observation that magnetic moments of magnetite/maghemite nanoparticles are blocked for sizes exceeding 40–50 nm at the room temperature.

Back in 1996, Kirschvink formulated a hypothesis on the mechanism of transduction of the nonthermal electromagnetic energy by magnetite and underlined the need of a cellular-level dosimetric investigation in the very proximity of magnetite crystals in the brain [7].

The first ones to raise the question about a possible connection between “environmental levels” of magnetic ( $H$ ) field strength (arising from mobile phones radiation) and some possible deleterious biological effects were the group of Cranfield in 2003 [8]. However, in a second paper of the same group published soon after their first one [9], they reported that the magnetite-containing bacteria used as a target were not affected by  $H$  field of the radiofrequency (RF) radiation emitted by mobile phone.

A second wave of concern, connected to effects of  $H$ -component of “environmental levels” of electromagnetic fields, was signaled by the publication in 2014 of a paper by Engels et al. [10] who reported that a species of migratory birds, European robins (*Erithacus rubecula*), when being exposed to the background electromagnetic noise in the frequency range 50 kHz–5 MHz, were not able to orient anymore based on their magnetic compass in the brain. The study, which was completely double-blinded, also demonstrated that the effect of anthropogenic electromagnetic noise on the behavior of birds was reproducible.

In 2009, Milham even raised the hypothesis that there was a connection between firemen cancers cases and the use of portable radio transceivers used in front of the face [11].

With aforementioned gathered biological data, it becomes evident that  $H$ -field component needs a more careful consideration, especially when RF dosimetry is applied in tissues containing magnetic materials.

An early but rare approach in the direction of  $H$ -field RF dosimetry was made by Kuster and Balzano in 1992 [12], who analyzed electromagnetic energy deposition generated by  $H$ -field component. The idea was re-launched in 2015 by Rubtsova et al. [13] in connection to exposure assessments in the near field of personal wireless telecommunication devices.

Present approach proposes that in some specific exposure cases, to express specific absorption rate (SAR) of energy deposition in human tissues (heating) by taking into account both contributions: the one due to the electric ( $E$ ) field, (SAR $_E$ ), and the one due to  $H$ -field, (SAR $_H$ ). Presently, the general rule is to report only SAR $_E$  value, because human tissues are considered as dielectric materials, without having magnetic properties. Consequently, experimental RF dosimetry makes use of only  $E$ -field probes, but not  $H$ -field probes.

SAR $_E$  can be calculated by the formula [14]:

$$\text{SAR}_E = \sigma * E^2 / \rho \quad (1)$$

where  $\sigma$  is the electrical conductivity of the tissue,  $E$  the root-mean-square (rms) value of  $E$ -field strength inside the tissue and  $\rho$  the mass density of the tissue. Alternatively, SAR $_E$  may be expressed as [14]:

$$\text{SAR}_E = c * dT/dt \quad (2)$$

where  $c$  is its specific heat of the targeted material/tissue and  $dT/dt$  the temperature increment induced by the electromagnetic exposure.

With the new data indicating three orders of magnitude more ferrimagnetic material (magnetite/maghemite) present in the human brain, as reported in September 2016 [5] compared with previous data, it becomes interesting to assess SAR $_H$  separately, based on  $H$ -field heating contribution. It is known that the brain functions are particularly sensitive to temperature increase, a deviation from the normothermal state by 1°C being able to affect the oxygen affinity of hemoglobin and the rate of chemical reactions, with all the consequences. That is why we consider that brain heating due to magnetic-component of RF field deserves a special attention in the context.

The magnetic properties of human brain tissue were well modeled by a combination of ferrihydrite (often encountered as ordered nanoparticles — yet exhibiting a pronounced ferrimagnetism) and

magnetite nanoparticles, also ferrimagnetic [15]. Therefore, in order to express SAR<sub>H</sub> we will use here a dosimetric approach inspired from the area of hyperthermia induced by RF absorption in magnetic liquids. SAR<sub>H</sub> in such a liquid can be expressed in two ways, based on either internal value of  $H$ -field strength or temperature increase during the exposure [16]:

$$\text{SAR}_H = P/m = 2\pi * \mu_0 * f * H^2 * \chi'' / (\rho_s * \Phi_M) \quad (3)$$

$$\text{SAR}_H = (c * V_s / m) * (dT/dt) \quad (4)$$

where  $P$  is the dissipated power,  $\rho_s$  the mass density of magnetic nanoparticle (solid phase in the ferrofluid),  $\mu_0$  the vacuum permeability,  $f$  the field frequency,  $H$  the rms value of the magnetic field strength inside the sample,  $\chi''$  the imaginary part of the complex magnetic susceptibility,  $\Phi_M$  the fraction of magnetic particles in suspension,  $c$  the specific heat capacity of the sample,  $m$  the mass of the magnetic particles,  $V_s$  the total volume of the liquid containing the nanoparticles and  $dT/dt$  the temperature increment.

In the case of brain tissue treated as a ferrimagnetic material, it is therefore cautious to express total SAR as the sum of both SAR components:

$$\text{SAR} = \text{SAR}_E + \text{SAR}_H \quad (5)$$

For a realistic assessment of thermal dosimetry in the brain, it is however necessary to consider the more complex approach of heating process, which takes into account the metabolism, heat conduction and blood flow. External origin of heat contribution of SAR superimposes to these terms. The bioheat transfer equation of Pennes governing the energetic equilibrium during RF exposure was implemented in 2016 for a homogeneous model of human brain [17], but not considering SAR<sub>H</sub> contribution. The analysis of the effect of used values of thermal parameters on the overall temperature distribution in the brain showed that: a) arterial blood temperature plays the most significant role in the cerebral temperature distribution; b) the dominant thermophysiological factor influencing temperature increase is the blood perfusion rate; c) temperature rise is just slightly influenced by the heat transfer coefficient and by the heat conductivity. However, it is stated that the computational human thermal modeling studies have suffered to date from lack of reliable data on blood flow [18] — which is proved to be crucial for a realistic temperature increase assessment. Early in 2017, the authors of [18] incorporated the measured blood flow values in a computational bioheat thermal model of the human head and reported that peak temperature elevation due to individual and regional variations in the blood flow did not exceed  $\pm 15\%$ .

Based on these latest findings, present research aims at SAR determination in a more simplified model, which does not take into account the Pennes bioheat equation. The particular situation of SAR assessment refers to the case when a portable transceiver is used in front of the face. Such devices emit radiation in the very high or ultra high frequency ranges and are used either in some occupations (firefighters, policemen, guardians, etc.) or by radio-amateurs. RF energy is absorbed and may heat up tissues, depending on the emitted power, on the distance they are kept from the face and on the peculiarities of the biological tissues.

Portable RF transceivers are designed to emit at high output powers — of maximum 5 W (or, for some models, even 8 W) and are equipped with rubber ducky antennas, which, as short whips, have a near field dependent on the current distribution in the pitched helix antenna, current that may produce very intense localized  $H$ -fields. Being kept at distances of the order of 5–10–15 cm in front of the face/head, the safe use of portable transceivers may be critical.

By experiments and calculation, we aim to estimate the  $H$ -field contribution to SAR for a face-held transceiver. The emitted field impinges the skull and penetrates brain tissues which are sprinkled by magnetite crystals. Absorbing RF field by  $H$ -component, they will increase energy (and temperature) at levels which were neglected up to now. By using simplified suppositions and a water-based magnetic fluid to simulate the brain magnetic composition, it was possible to make a gross approximation of SAR<sub>H</sub> order of magnitude, based on thermal measurements and on estimative calculations.

## 2. NEAR FIELD EXPOSURE AND ENERGY DEPOSITION IN BRAIN DUE TO RADIATION EMITTED BY A PORTABLE TRANSCEIVER

### 2.1. Field Source Description

In the present experiment, we use a two-way transceiver model UV-B5 BaoFeng Amateur Portable Radio (dual band) operating on the frequency  $f = 446$  MHz with frequency modulation telephony signal in a channel of 12.5 kHz. The transceiver is equipped with a rubber ducky antenna with inner (metallic) length of 11.5 cm and helix diameter of 2.8 mm. This type of antenna is difficult to characterize electrically because the current distribution along it is not sinusoidal. The output power does not give significant information, but rather the current in it and the total radiated power.

### 2.2. Near Field in Air

The exposimetric characterization was made by separately measuring both field strengths,  $E$ - and  $H$ -fields in air, in the vicinity of the device, in real-life conditions. We used an ESM-30 RADMAN XT exposimeter (Narda Safety Test Solutions, Germany) with data logging facility and RADMAN ESM-TS software (Fig. 1). The exposimeter has two tiny  $E$ - and  $H$ -field sensors, a few millimetres in diameter, placed at a distance of 4.5 cm from each other (the typical deviation =  $\pm 3$  dB at the measured frequency). Magnitudes of local field strengths were obtained after three orthogonal measurements were made in each point, so as to obtain an omnidirectional result. Field levels expressed by exposimeter were posted in a log file in the form of percentage from ICNIRP reference levels of occupational exposure [19]. Therefore, we had to transform percentages in absolute field strengths.



**Figure 1.** Portable transceiver, magnetic liquid sample to simulate magnetite presence in the brain, fluoroptic probe immersed to measure heating for magnetic-dosimetry, RADMAN XT exposimeter to measure incident field strength and TrueTemp3 software on laptop to record temperature increase.

The transceiver was held vertically, as usually used in front of the face. Field strength measurements for present experiment were made only along a perpendicular line ( $Oz$ , Fig. 1) puncturing the device surface at a height  $H = 11.5$  cm from its bottom. The distance  $D$  on horizontal direction from the transceiver surface was varied between 2 cm and 20 cm (near field zone), corresponding to positions where human head was present during use. The height  $H$  at which we measured the fields in air corresponds in to the basis of the rubber ducky antenna (where usually stays the forehead).

Field strengths variations with distance are presented in Fig. 2. At  $D = 10$  cm from the transceiver's surface for example, rms field strengths are:  $E = 22.5$  V/m and  $H = 0.22$  A/m. While  $E$ -field strength is much lower than the safety limit for population (of 63.3 V/m),  $H$ -field exceeds even occupational safety limit (of 0.17 A/m) by 30% [19]. However, in the technical booklet of the BaoFeng transceiver, the producer advises the user to hold the device in vertical position with microphone at 3–4 cm away from the lips. As we may observe, at  $D = 4$  cm,  $H$ -field in air exceeds occupational safety limit by 65%.

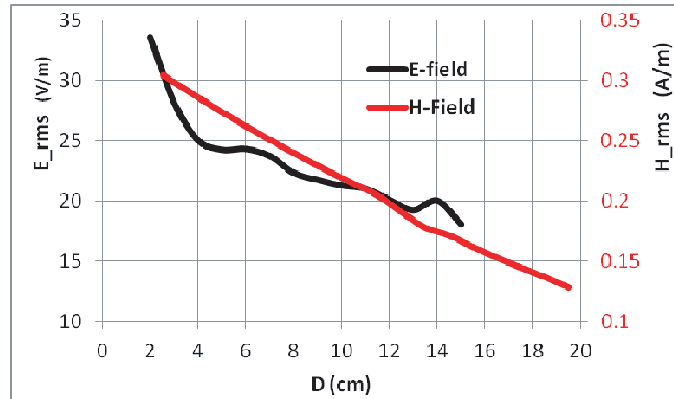


**Figure 2.** Electric and magnetic field strengths in air versus distance, in the proximity of the portable transceiver, in a horizontal direction situated at a height of 11.5 cm from the device bottom. Output power of the rubber ducky antenna was 5 W.

### 2.3. Specific Absorption Rate, SAR<sub>E</sub>, Measured by E-Field Probe

An experimental dosimetric quantification was made, following standardized methodology presented in [20, 21] but solely from the perspective of  $E$ -field absorption effect. Practically, a set of dosimetric measurements were made for BaoFeng transceiver, from which we select here one result that contributes to present analysis.

SAR<sub>E</sub> was determined in brain-simulating liquid filling an elliptic flat phantom while the transceiver was operated at 5 W and at 100% duty cycle (continuous emission). Dielectric properties of the simulating brain liquid at  $f = 446$  MHz were: relative dielectric constant  $\epsilon'_r = 43.48$ ; electric conductivity  $\sigma = 0.87$  S/m. The SAR test bench operated in an electromagnetically shielded room. It was a SATIMO-COMOSAR Twin model controlled by OPENSAR software which also provided data processing.  $E$ -field probe was a triple dipole model EP96 produced by SATIMO, offering an omnidirectional response.

When the transceiver was placed at  $D = 4$  cm from the flat phantom's shell (Fig. 3), SAR<sub>E</sub> distribution was obtained in a longitudinal plane containing the maximum SAR value, looked like in Fig. 4. It is observed that local peak SAR<sub>E</sub> values range covers the interval (7.44–7.96) W/kg. The averaged SAR<sub>E</sub> over 10 g of tissue (as in standard used in Europe [19]) is 6.95 W/kg, value which significantly exceeds the safety limit for the head in case of public exposure — of 2 W/kg and approaches the occupational safety limit — of 10 W/kg. This situation corresponds to a measured  $E$ -field in air of 25 V/m, at the phantom shell limit, which does not exceed the protective limit for the general population. At  $D = 10$  cm, peak values of SAR<sub>E</sub> range cover the interval (0.94–1.34) W/kg, and the averaged SAR<sub>E</sub> over 10 g of tissue was 1.03 W/kg. These values ensure safety for general public. At this distance from the transceiver,  $D = 10$  cm, SAR<sub>H</sub> will be further assessed, based on available data in literature, to establish its separate contribution to possible co-heating of tissue similar-to-brain.

## 3. MAGNETIC FLUID CHARACTERISTICS AND ITS DOSIMETRIC RESPONSE TO THE TRANSCEIVER NEAR-FIELD

As shown above, the incident  $H$ -field strength in air exceeds the occupational safety limit at the distance  $D = 10$  cm from the transceiver. The question rises about the value of SAR<sub>H</sub> induced by this incident field impinging a liquid similar to the brain but also containing magnetite nanoparticles.

Generally in RF dosimetry, because brain tissue is considered non-magnetic, SAR<sub>H</sub> is completely neglected. With new discoveries of both endogenous and exogenous magnetic crystals in the human brain [3–5], SAR<sub>H</sub> should be also considered as a contributor to total SAR.

Therefore, below we will present measurements and calculations aimed to coarsely approximate the expected order of magnitude of SAR<sub>H</sub>. The main idea was to consider the interaction between the

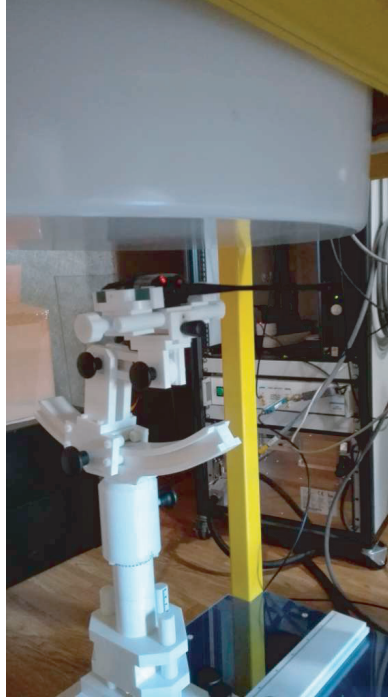


**Figure 3.** Portable transceiver placed below the flat phantom shell of SATIMO-COMOSAR dosimetric system, phantom filled with brain-simulating liquid for electric-dosimetric measurement.

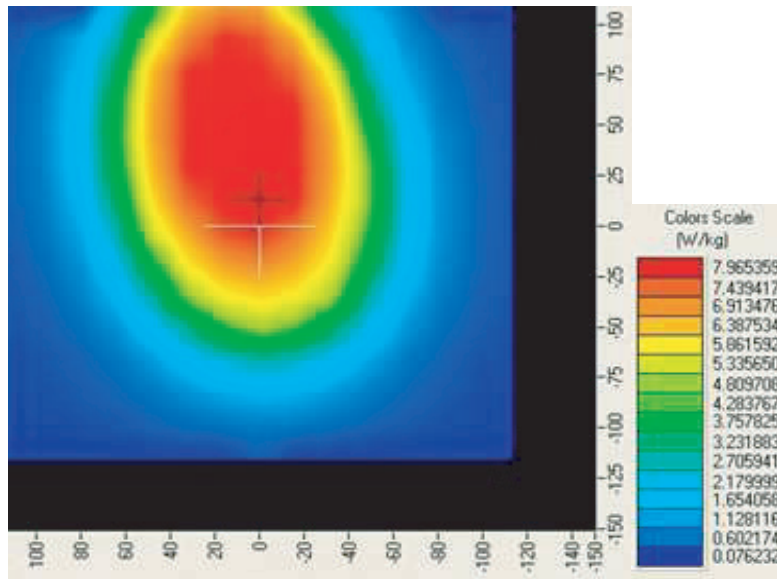


**Figure 4.** SAR<sub>E</sub> distribution measured in the flat phantom filled with brain simulating liquid, with portable transceiver distanced at 4 cm from the phantom's shell, parallel with it; output power = 5 W.

$H$ -field at 446 MHz and a magnetic liquid. Such a liquid should be however similar as much as possible to the dielectric properties of the simulating brain previously used in the measurement of SAR<sub>E</sub>.

We have therefore chosen two water-based magnetic fluid samples (denoted here by  $S1$  and  $S2$ ) containing magnetic nanoparticles coated by tetramethylammonium hydroxide ( $N(CH_3)_4OH$ ) and obtained by a chemical precipitation method [22]. They contain a mixture of magnetite and maghemite

particles, with an average diameter  $d$  approaching 10 nm (including the surfactant shell of the magnetite core). The average size of the magnetic core diameter —  $d_M$ , volume fraction of solid phase in suspension —  $\Phi$ , fraction of ferrophase in suspension —  $\Phi_M$ , particles' concentrations —  $n$ , and fluid density —  $\rho_F$  are specified in Table 1 [22].

The fluids contain a mixture of magnetic particles of various diameters: for  $S1$  diameters they vary between (4.8–16) nm, while for  $S2$  they vary between (3.4–14.2) nm. Such dimensions are smaller than diameters of crystals discovered in the brain. Transmission electron microscopy micrographs indicate that the particles in these samples are spherical [22], which means that they are not of the type of biogenic magnetite [23–25], but similar to the geometry of anthropogenic magnetite.

**Table 1.** Main characteristics of the magnetic fluid samples.

Sample no.	Characteristics					
	$d$ (nm)	$d_M$ (nm)	$\Phi$ (%)	$\Phi_M$ (%)	$\rho_F$ (kg/m <sup>3</sup> )	$n$ (part/m <sup>3</sup> )
$S1$	9.20	6.23	2.0	1.42	1021.4	$1.11 * 10^{23}$
$S2$	7.97	6.70	2.6	2.03	1060.5	$1.30 * 10^{23}$

These two magnetic liquid samples were exposed sequentially, in volumes of  $V_s = 2$  ml each, in front of the portable transceiver, at distance  $D = 10$  cm, at the measured incident magnetic field strength  $H = 0.22$  A/m in air.

The heating effect of the magnetic field was measured by a Luxtrone One fluoroptic probe (Luxtron Corp., USA) inserted in the liquid (Fig. 1). The probe tip is  $< 0.2$  mm and it was maintained in the same position for all measurement repetitions. TrueTemp3 software allowed recording of the temperature evolution every second. This fiber optic thermometer is very accurate, immune to RF fields and non-perturbative. It is based on a phosphorescent crystal and determines the temperature by measuring the decay time of its emitted light. Its resolution is 0.1 degrees C.

Exposure duration and temperature recording were applied continuously for 360 seconds and repeated 5 times for each magnetic fluid sample. A very good reproducibility of the results was obtained after smoothing the noisy signal and fitting the trend. An example of heating dynamics without radiation turned on (blue trace) and with  $H$ -field component of the radiated field impinging the magnetic liquid (red trace) is presented in Fig. 5. The fitting lines and their equations allowed the determination of temperature increment from differences between the two slopes.

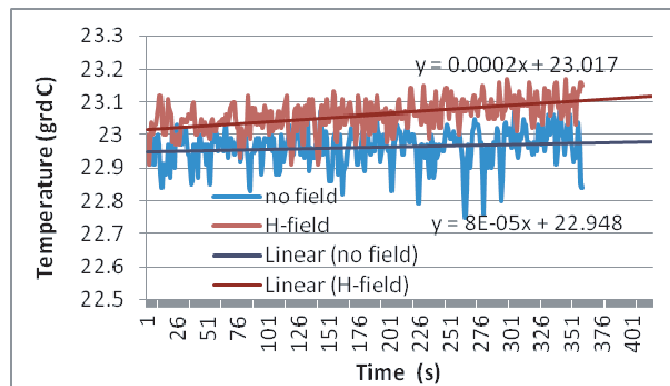


**Figure 5.** Temperature evolution in the magnetic liquid ( $S2$ ) without and with the field emitted by the portable transceiver as measured over 6 minutes by the fluoroptic probe at 10 cm distance from the device with the antenna output power of 5 W.

### 3.1. Specific Absorption Rate SAR<sub>H</sub> Measured by Fiber Optic Temperature Probe

Average temperature increments experimentally determined in each of the two magnetic liquid samples were:

$$(dT/dt)_{S1} = 1.5 \times 10^{-4} \text{ grdC/s} \quad (6)$$

$$(dT/dt)_{S2} = 1.4 \times 10^{-4} \text{ grdC/s} \quad (7)$$

The specific heat capacity of the sample,  $c$ , to be used in Eq. (4), can be well approximated by the formula recently demonstrated in [26]:

$$c = [(1 - \Phi) * \rho_L * c_L + \Phi * \rho_S * c_S] / [(1 - \Phi) * \rho_L + \Phi * \rho_S] \quad (8)$$

where:  $\rho_L$  is the density of the carrier liquid (water),  $c_L$  the specific heat of the liquid,  $\rho_S$  the density of the solid phase (nanoparticles), and  $c_S$  the specific heat of the solid material of nanoparticles (considered here as magnetite). We used next data:  $\rho_L = 1000 \text{ kg/m}^3$ ,  $c_L = 4180 \text{ J/kg}^*\text{K}$ ,  $\rho_S = 5200 \text{ kg/m}^3$ ,  $c_S = 670 \text{ J/kg}^*\text{K}$ . With these, the two specific heat values of the ferrofluid samples are:  $(c)_{S1} = 3843.2 \text{ J/kg}^*\text{K}$  and  $(c)_{S2} = 3752.2 \text{ J/kg}^*\text{K}$ .

In relation (4),  $V_s$  is 2 ml in both cases, while the mass of magnetic material in the samples can be calculated by:

$$m = V_s * \rho_S * \Phi_M \quad (9)$$

So we get:  $(m)_{S1} = 147.7 \mu\text{g}$  magnetite and  $(m)_{S2} = 211.1 \mu\text{g}$  magnetite. With these magnetite quantities, the magnetic concentrations of the liquids  $S1$  and  $S2$  are:  $C1 = 72.3 * 10^3 \mu\text{g}$  magnetite/g of solution and respectively  $C2 = 99.5 * 10^3 \mu\text{g}$  magnetite/g of solution. If comparing against the content of exogenic magnetite in human brain reported in September 2016 [5], of 0.2–12  $\mu\text{g}$  magnetite/g of dry brain tissue, we have approximately 3 orders of magnitude higher concentrations of ferrimagnetic material in our solutions. However, the dimensions of the particles are in the lowest limit of real particles dimensions in the brain (one order of magnitude smaller). Besides, not only concentration and dimensions of particles influence the rate of heat production by RF absorption, but much more factors — which will be discussed in the last part of the paper.

Inserting the numerical values in relation (4), we receive the expected SAR<sub>H</sub> in the case of the two ferrofluid samples:

$$(\text{SAR}_H)_{S1} = 7.8 \text{ mW/kg} \quad (10)$$

$$(\text{SAR}_H)_{S2} = 5 \text{ mW/kg} \quad (11)$$

These values are two and a half orders of magnitude lower than SAR<sub>E</sub>.

### 3.2. Specific Absorption Rate SAR<sub>H</sub> Assessed by Calculation

While using relation (3), we need to know the  $H$ -field strength, not in air, but inside the ferrofluid. In order to do this, we suppose here an idealised case — a plane wave penetrating and attenuating like in a planar half-space filled by liquid, not taking into account the shape and dimensions of the magnetic sample. With this supposition,  $H$ -field magnitude variation with depth  $z$  in the fluid will be of the form:

$$H(z) = H_{inc} * e^{-\alpha * z} \quad (12)$$

where  $H_{inc}$  is here the rms field strength measured in air at the interface with the magnetic liquid (in our case  $H_{inc} = 0.22 \text{ A/m}$ ), and  $\alpha$  is the wave attenuation constant [27, 28]:

$$\alpha = \pi * f * \text{sqrt}(\mu_0 \varepsilon_0) * \text{sqrt} \left\{ 2 * \left[ \text{sqrt} \left( (\mu'^2 + \mu''^2) * (\varepsilon'^2 + \varepsilon''^2_{eff}) \right) - (\mu' \varepsilon' - \mu'' \varepsilon''_{eff}) \right] \right\} \quad (13)$$

where sqrt is the square root function,  $\mu_0$  the vacuum magnetic permeability,  $\varepsilon_0$  the vacuum electrical permittivity, and  $\mu'$ ,  $\mu''$ ,  $\varepsilon'$ ,  $\varepsilon''_{eff}$  are the real and imaginary parts of the relative complex magnetic permeability and electric permittivity respectively, with the observation that:

$$\varepsilon''_{eff} = \varepsilon'' + \sigma / (\omega * \varepsilon) \quad (14)$$

with  $\sigma$  — the electrical conductivity and  $\omega$  — the field pulsation. Approximative values were extracted for an average sample between  $S1$  and  $S2$  (they are very similar). So, for our material, parameters

mentioned above were extracted from [27, 29]:  $\mu' = 1.5$ ,  $\mu'' = 0.02$  and from [27] respectively:  $\varepsilon' = 50$ ,  $\varepsilon''_{eff} = 125$ . Inserting these values into relation (12) we get the internal  $H$ -field strength in the ferrofluid:

$$H(z) = 0.22 * e^{-70*z} \text{ (A/m)} \quad (15)$$

For  $z = 8$  mm (the depth in  $Oz$  direction where the temperature probe's tip was immersed in the liquid during SAR<sub>H</sub> measurements), the rms value of internal magnetic field will be  $H = 0.13$  A/m. With this value inserted in relation (3) and choosing an average imaginary part of the complex magnetic susceptibility  $\chi'' = 0.15$  from [30], we finally get SAR<sub>H</sub> = 50 mW/kg.

To resume, SAR<sub>H</sub> absolute contribution in the experimental case presented above is in the order of a few units or tens of mW/kg.

Because different configurations were used for SAR<sub>E</sub> and SAR<sub>H</sub> calculations, and taking into account that electromagnetic field penetration inside an exposed body is highly dependent on the shape, dimensions and electric/magnetic properties of that body, the comparison between SAR<sub>E</sub> and SAR<sub>H</sub> when the two quantities were determined in different conditions are improper to be made. Local temperature increment in the measurement position of the tip of fluoroptic probe may not be sufficient for an overall view of the magnetic heating. Therefore, a precise assessment of SAR<sub>H</sub> contribution to total SAR in the case of human brain with ferrimagnetic crystals content can be made by numerical dosimetry with modified simulating liquids than currently in use.

#### 4. DISCUSSION ON SAR ESTIMATION IN CASE OF TISSUES PRESENTING MAGNETIC PROPERTIES

In 2002, Rosenweig established the equation describing power dissipation in magnetic fluids exposed to RF fields [31]. The power generated in iron oxide nanoparticles was proportional to the square of the applied  $H$ -field strength. In consequence, the thermal energy dissipating in a tissue containing magnetic particles and quantified by SAR<sub>H</sub> will be also proportional to  $H^2$ , for a fixed frequency and for a fixed situation — as shown by relation (3).

If we would aim to express the incident  $H$ -field for which the safety limit of SAR would be reached in our experimental case, we could easily obtain it by using relations (3), (5), (12) and (15). Relation (3) is a direct consequence of Rosenweig's equation. By considering that SAR<sub>H</sub> contribution is half of total SAR, we would have two situations: public safety limit (SAR<sub>limit</sub> = 2 W/kg) and occupational safety limit (SAR<sub>limit</sub> = 10 W/kg). In consequence  $H$ -field in air, at  $D = 10$  cm from the transceiver, should have next values: a) public  $H_{limit} = 2.97$  A/m; b) occupational  $H_{limit} = 6.08$  A/m. If we compare these values against the analyzed experimental situation, we find that we would need 13.5 times and respectively 27.6 times higher  $H$ -field strength to pose a health risk.

A very significant aspect to be certainly considered in a discussion is connected to the factors that affect heat generation in ferrimagnetic nanoparticles dispersions. It has been very recently proved that the mechanism of heating is highly dependent on multiple factors [32–35]: a) magnetic particle sizes (and in correlation with field frequency); b) nanoparticles compositions; c) particle concentrations; d) magnetic fluid viscosity; e) particle's surface; f) shape anisotropy; g) interface exchange anisotropy; h) dipolar interactions. It is demonstrated that particles sizes influence the types of relaxation processes that conduct magnetic heating. The increase of solution viscosity leads to a decrease of heating rate. Increasing the anisotropy leads to the increase of relaxation time. The shape and magnetocrystalline anisotropy of particles prove to be the key parameters in tuning the magnetic hyperthermia.

On the other hand, in 2012 an interesting biasing effect of  $H$ -field was reported regarding the dielectric properties of magnetic fluids at hundreds of MHz–GHz frequency range [36]. The phenomena materialise in the increase of  $\varepsilon'$  and  $\varepsilon''$  values when incident  $H$  field increases, and in a shift of the peak of dielectric parameters values to lower frequencies, when the  $H$  field increases.

In such complex circumstances in which scientific research is ongoing on this topic, realistic impact on human brain of  $H$ -field component of RF radiation, provided by face-held transceivers at different frequencies, remains a challenging issue.

## 5. CONCLUSION

Present work aims at considering  $H$ -field component contribution to total electromagnetic energy deposition in the human head when taking into account new-discovered high content of ferrimagnetic nanoparticles in the brain. RF field emitted by rubber ducky antenna of transceivers usually used at few centimeters in front of the face, at output powers of 5–8 W, may produce incident  $H$ -field strengths in air which exceed safety limits for public and even for professionals. It becomes therefore obligatory to take into account the magnetic heating of tissues in the head as well, besides “classical” dielectric heating contribution. It was within reach to adapt magnetic hyperthermia knowledge to magnetic RF dosimetry of wireless communication devices. By such means we propose here a preliminary and original dosimetric demarche that enables determination of the order of magnitude of magnetic-SAR.

In the first stage, we measured the standardized electric-SAR in a flat phantom filled with dielectric liquid simulating average brain properties. This step provided the order of magnitude expected for SAR $_E$  due to near-field electric-component of the antenna. In the second stage, by a fluoroptic temperature probe and by calculations inspired from microwave hyperthermia of ferrimagnetic nanoparticles, the order of magnitude of SAR $_H$  due to near-field magnetic-component of the antenna was determined. A number of simplifying suppositions were used, while the brain-simulating liquids in the two cases (except of magnetite nanoparticles presence) were not identical in the two stages. That is why comparison between the two contributions is just orientative.

Future work will focus on computational RF dosimetry devoted to analysis of SAR due to devices/antennas impacting with significant  $H$ -field component in the proximity of tissues with significant ferrimagnetic content, like human brain, when it is polluted by anthropogenic magnetic crystals deposited from the environment.

## ACKNOWLEDGMENT

The authors are grateful to Dipl.-Eng. Ion Patru, Dipl.-Eng. Ionel Dumbrava and Dipl.-Eng. Viorica Voicu from the National Institute for Research, Development and Testing in Electrical Engineering (ICMET) in Craiova, Romania, for the electric SAR measurements they made in their accredited laboratory.

## REFERENCES

1. Kirschvink, J. L., A. Kobayashi-Kirschvink, and B. J. Woodford, “Magnetite biomineralization in the human brain,” *Proceedings of the National Academy of Sciences of the United States of America*, Vol. 89, No. 16, 7683–7687, 1992.
2. Sant’Ovaia, H., G. Marques, A. Santos, C. Gomes, and A. Rocha, “Magnetic susceptibility and isothermal remanent magnetization in human tissues: A study case,” *Biometals*, Vol. 28, 951–958, 2015.
3. Collingwood, J. F. and N. D. Telling, “Iron oxides in the human brain,” *Iron Oxides: From Nature to Applications*, Faivre D. (Ed.), 143–176, Wiley-VCH Verlag GmbH & Co. KgaA, 2016.
4. Stormer, F. C., “Magnetite in dura and pia mater in the brain. A shield against electromagnetic fields?,” *Medical Hypotheses*, Vol. 82, 122–123, 2014.
5. Maher, B. A., I. A. M. Ahmed, V. Karloukovski, D. A. MacLaren, P. G. Foulds, D. Allsop, D. M. A. Mann, R. Torres-Jardón, and L. C. Calderon-Garciduenas, “Magnetite pollution nanoparticles in the human brain,” *Proceedings of the National Academy of Sciences of the United States of America*, Vol. 113, No. 39, 10797–10801, Sep. 2016.
6. Kumar, P., M. Bulk, A. Webb, L. van der Weerd, T. H. Oosterkamp, M. Huber, and L. Bossoni, “A novel approach to quantify different iron forms in ex-vivo human brain tissue,” *Scientific Reports*, Vol. 6, 38916, 2016, DOI: 10.1038/srep38916.
7. Kirschvink, J. L., “Microwave absorption by magnetite: A possible mechanism for coupling nonthermal levels of radiation to biological systems,” *Bioelectromagnetics*, Vol. 17, 187–194, 1996.

8. Cranfield, C. G., H. G. Wieser, J. Al. Maddan, and J. Dobson, "Preliminary evaluation of nanoscale biogenic magnetite-based ferromagnetic transduction mechanisms for mobile phone bioeffects," *IEEE Transactions on NanoBioscience*, Apr. 2003.
9. Cranfield, C. G., H. G. Wieser, and J. Dobson, "Exposure of magnetic bacteria to simulated mobile phone-type RF radiation has no impact on mortality," *IEEE Transactions on NanoBioscience*, Vol. 2, No. 3, 146–149, 2003.
10. Engels, S., N.-L. Schneider, N. Lefeldt, C. M. Hein, M. Zapka, A. Michalik, D. Elbers, A. Kittel, P. J. Hore, and H. Mouritsen, "Anthropogenic electromagnetic noise disrupts magnetic compass orientation in a migratory bird," *Nature*, Vol. 509, 353, May 15, 2014.
11. Milham, S., "Most cancer in firefighters is due to radio-frequency radiation exposure not inhaled carcinogens," *Medical Hypotheses*, Vol. 73, 788–789, 2009.
12. Kuster, N. and Q. Balzano, "Energy absorption mechanism by biological bodies in the near field of dipole antennas above 300 MHz," *IEEE Transactions on Vehicular Technology*, Vol. 41, No. 1, 17–23, 1992.
13. Rubtsova, N., S. Perov, O. Belaya, N. Kuster, and Q. Balzano, "Near field radiofrequency electromagnetic exposure assessment," *Electromagnetic Biology and Medicine*, Vol. 34, No. 3, 180–182, 2015.
14. Durney, C. H., H. Massoudi, and M. F. Lskander (eds.), *Radiofrequency Radiation Dosimetry Handbook*, 4th Edition, Armstrong Laboratory (AFMC), Occupational and Environment Directorate, Radiofrequency Radiation Division, Brooks Air Force Base, TX, USA, 1986.
15. Brem, F., L. Tiefenauer, A. Fink, J. Dobson, and A. M. Hirt, "A mixture of ferritin and magnetite nanoparticles mimics the magnetic properties of human brain tissue," *Physical Review B*, Vol. 73, 224427, 2006.
16. Liu, X. L., H. M. Fan, J. B. Yi, Y. Yang, E. S. G. Choo, J. M. Xue, D. D. Fana, and J. Ding, "Optimization of surface coating on Fe<sub>3</sub>O<sub>4</sub> nanoparticles for high performance magnetic hyperthermia agents," *Journal of Materials Chemistry*, Vol. 22, 8235–8244, 2012.
17. Cvetkovic, M., D. Poljak, and A. Hirata, "The electromagnetic-thermal dosimetry for the homogeneous human brain model," *Engineering Analysis with Boundary Elements*, Vol. 63, 61–73, 2016.
18. Laakso, I., R. Morimoto, A. Hirata, and T. Onishi, "Computational dosimetry of the human head exposed to near-field microwaves using measured blood flow," *IEEE Transactions on Electromagnetic Compatibility*, Vol. 59, No. 2, 739–746, 2017.
19. International Commission on Non-Ionizing Radiation Protection (ICNIRP), "Guidelines for limiting exposure to time varying electric, magnetic, and electromagnetic fields," *Health Physics*, Vol. 74, 494–522, 1998.
20. International Electrotechnical Commission (IEC), "Procedure to measure the specific absorption rate (SAR) for hand-held mobile wireless devices in the frequency range of 300 MHz to 3 GHz," *IEC62209*, Geneva, Switzerland, 2001.
21. International Electrotechnical Commission (IEC), "Human exposure to radio frequency fields from hand-held and body-mounted wireless communication devices — human models, instrumentation, and procedures — Part 2: Procedure to determine the specific absorption rate (SAR) in the head and body for 30 MHz to 6 GHz handheld and bodymounted devices used in close proximity to the body," *TC/SC106/90/NP*, Geneva, Switzerland, 2005.
22. Racuciu, M., D. E. Creanga, A. Airinei, and V. Badescu, "Synthesis method influence on water based magnetic fluid properties," *J. Optoelectr. Adv. Mat.*, Vol. 10, No. 3, 635–638, Mar. 2008.
23. Giere, R., "Magnetite in the human body: Biogenic vs. anthropogenic," *Proceedings of the National Academy of Sciences of the United States of America*, Vol. 113, No. 43, 11986–11987, Oct. 2016.
24. Strbak, O., P. Kopcansky, M. Timko, and I. Frollo, "Single biogenic magnetite nanoparticle physical characteristics — A biological impact study," *IEEE Transactions on Magnetics*, Vol. 49, No. 1, 457–462, Jan. 2013.
25. Strbak, O., P. Kopcansky, M. Timko, and I. Frollo, "Correction to: Single biogenic magnetite nanoparticle physical characteristics. A biological impact study," *IEEE Transactions on Magnetics*,

- Vol. 49, No. 9, 1–3, Sept. 2013.
26. Marin, C. N., I. Malaescu, and P. C. Fannin, “Theoretical evaluation of the heating rate of ferrofluids,” *Journal of Thermal Analysis and Calorimetry*, Vol. 119, No. 2, 1199–1203, Feb. 2015.
  27. Fannin, P. C., I. Malaescu, C. N. Marin, and N. Stefu, “Microwave propagation parameters in magnetic fluids,” *European Physics Journal*, Vol. E 29, 299–303, 2009.
  28. Malaescu, I., C. N. Marin, P. C. Fannin, N. Stefu, A. Savici, and D. Malaescu, “Comparative study of the microwave propagation parameters of some magnetic fluids in the presence of polarizing field,” *American Institute of Physics Conference Proceedings*, Vol. 1387, 208, 2011.
  29. Yun, H., X. Liu, T. Paik, D. Palanisamy, J. Kim, W. D. Vogel, A. J. Viescas, J. Chen, G. C. Papaefthymiou, J. M. Kikkawa, M. G. Allen, and C. B. Murray, “Size- and composition-dependent radio frequency magnetic permeability of iron oxide nanocrystals,” *American Chemical Society Nano*, Vol. 8, No. 12, 12323–12337, 2014.
  30. Malaescu, I., C. N. Marin, M. Bunoiu, P. C. Fannin, N. Stefu, and L. Iordaconiu, “The effect of particle concentration on the heating rate of ferrofluids for magnetic hyperthermia,” *Analele Universitatii de Vest, Timisoara*, Vol. LVIII, Seria Fizică, 81–88, 2015.
  31. Rosenweig, R. E., “Heating magnetic fluid with alternating magnetic field,” *Journal of Magnetism and Magnetic Materials*, Vol. 252, 370–374, 2002.
  32. Shah, R. R., T. P. Davis, A. L. Glover, D. E. Nikles, and C. S. Brazel, “Impact of magnetic field parameters and iron oxide nanoparticle properties on heat generation for use in magnetic hyperthermia,” *Journal of Magnetism and Magnetic Materials*, Vol. 387, 96–106, 2015.
  33. Obaidat, I. M., B. Issa, and Y. Haik, “Magnetic properties of magnetic nanoparticles for efficient hyperthermia,” *Nanomaterials*, Vol. 5, 63–89, 2015.
  34. Jazirehpour, M. and S. A. Seyyed Ebrahimi, “Synthesis of magnetite nanostructures with complex morphologies and effect of these morphologies on magnetic and electromagnetic properties,” *Ceramics International*, Vol. 42, 16512–16520, 2016.
  35. Jazirehpour, M. and S. A. Seyyed Ebrahimi, “Effect of aspect ratio on dielectric, magnetic, percolative and microwave absorption properties of magnetite nanoparticles,” *Journal of Alloys and Compounds*, Vol. 638, 188–196, 2015.
  36. Couper, C., C. N. Marin, and P. C. Fannin, “Biasing field effect on the microwave dielectric properties of magnetic fluids,” *Physics Procedia*, Vol. 9, 58–62, 2010.